On Robust Rectification for Uncalibrated Images

Francesco Isgrò and Emanuele Trucco
Department of Computing and Electrical Engineering
Heriot-Watt University, Edinburgh, UK
{fisgro,mtc}@cee.hw.ac.uk

Abstract

We present a robust algorithm performing uncalibrated rectification which does not require explicit computation of the epipolar geometry, and specifically of the fundamental matrix. Our algorithm exploits the fact that the fundamental matrix of a pair of rectified images has a particular, known form. This allows us to set up a minimization that yields the rectifying homographies directly from image correspondences. Experimental results show that our method works even in the presence of noise, and can cope with inaccurate point correspondences. Robustness in the presence of wrong point correspondences is also addressed in this paper, and a two steps outlier detector is described.

1 Introduction

The cornerstone for stereo and motion 2-frame analysis is the solution of the *correspondence problem* which can be synthesized as determining which parts of two images, say $\mathbf{I}_1$ and $\mathbf{I}_2$, are projections of the same scene element. The solution of this problem is given by a correspondence map, or equivalently a *disparity map*, which relates each pixel of $\mathbf{I}_1$ to at most one pixel in $\mathbf{I}_2$. In order to determine the correspondence map for each pixel $\mathbf{p}_1$ in $\mathbf{I}_1$ a pixel $\mathbf{p}_2$ maximizing a similarity measure must be determined [2]. The geometry of a stereo system, called *epipolar geometry* and codified in the fundamental matrix $\mathbf{F}$ [22], is such that correspondent points are constrained to lie on particular lines called *epipolar lines* [4]. Therefore if the fundamental matrix $\mathbf{F}$ is known the correspondence problem is reduced from a 2D search to a 1D search problem.

Needless to say, the search for a correspondent point can be simplified if the two images are warped [21] in such a way that the correspondent points lie on the same scan-line in the two images. In other words, the epipolar lines are parallel to the horizontal image axes. Note that most of the stereo algorithms presented in the literature assume this configuration. This process is called *rectification*, and the two transformed images can be regarded as obtained by a stereo rig obtained rotating the two original cameras.

The concept of rectification has been known for long to photogrammetrists [19], and their approach was merely optical. Most of the approach by vision researchers, like the ones presented by Ayache and Hansen [3], and Fusiello et al [5], assume that the two projection matrices are known. Only recently algorithms not assuming a full calibration of the two cameras, but only a weak calibration (knowledge of the epipolar geometry) have been presented [14, 17, 12]. In particular, Hartley [8] gives a theoretical presentation of uncalibrated rectification. All these algorithms rely on the estimation of the fundamental matrix $\mathbf{F}$. Despite the fact that several methods for computing the fundamental matrix have been published [10, 22], no algorithm has proved to be stable in every situation [10], making this a still open topic of research.

In this paper we present a novel algorithm performing projective rectification which does not require explicit computation of the epipolar geometry, and specifically of the fundamental matrix. We exploit the fact that the fundamental matrix of a pair of rectified images has a particular, known form to set up a minimization yielding the rectifying homographies *directly* from image correspondences. The two transformations computed by our algorithm can then be used to estimate the epipolar geometry between the two original images. Our algorithm makes use of theoretical results presented in [8]. A different version of this algorithm has been already presented in [9].

In the following subsection our notation is given. In the second section the epipolar geometry of a rectified stereo pair is characterized. Some results on the rectifying transformations are reviewed in the third section. The rectification algorithms is presented in the fourth section and experimental results are given in the fifth section. The last section is dedicated to final remarks and a brief discussion.

1.1 Notation

It is convenient to cast our presentation from the point of view projective geometry [18], whereby the image planes are considered as projective planes, and image points are represented as 3D column vectors. A rectifying transformation is a linear one to one transformation of the projective plane, called *homography*, represented by a 3×3 non-singular matrix.

We indicate column vectors by bold lower-case letters, such as $\mathbf{a}$. Row vectors are denoted by transposed column vectors, e.g., $\mathbf{a}^t$. Matrices are denoted by bold upper-case letters, e.g., $\mathbf{M}$. Scalars are denoted by italic letters.

Given a vector $\mathbf{a} = [a, b, c]^t$ we denote by $[\mathbf{a}]_\times$ the rank-2 skew-symmetric matrix used in place of the vector product by $\mathbf{a}$,

$$\begin{bmatrix} 0 & -c & b \\ c & 0 & -a \\ -b & a & 0 \end{bmatrix}$$

2 The epipolar geometry of two rectified images

It is well known that any two corresponding image points ($\mathbf{p}_1$,$\mathbf{p}_2$) are related via the fundamental matrix $\mathbf{F}$ by the algebraic relation

$$\mathbf{p}_1^t \mathbf{F} \mathbf{p}_2 = 0. \tag{1}$$

$\mathbf{F}$ is defined up to a scale factor and usually computed from 8 or more point correspondences using linear [7] or more accurate nonlinear methods [22]. If we interpret $\mathbf{F}\mathbf{p}_2$ as a line in the projective plane, equation (1) tells us that $\mathbf{p}_1$ is constrained to lie on $\mathbf{F}\mathbf{p}_2$, the epipolar line of $\mathbf{p}_2$ in $\mathbf{I}_1$ (the epipolar line of $\mathbf{p}_1$ in $\mathbf{I}_2$ is given by $\mathbf{F}^t\mathbf{p}_1$). The null spaces of $\mathbf{F}$ and $\mathbf{F}^t$ define the epipoles in the projective plane, $\mathbf{e}_1$ and $\mathbf{e}_2$, geometrically the projections on the two image planes of the centers of projection of the cameras. It can be proven [8] that $\mathbf{F}$ can be factorized as $[\mathbf{e}_1]_\times \mathbf{M}$, where $\mathbf{M}$ is a three-parameter family of non-singular matrices. Moreover, $\mathbf{M}$ is such that $\mathbf{M}\mathbf{e}_2 = \mathbf{e}_1$ and for each point $\mathbf{p}_2$ the point $\mathbf{M}\mathbf{p}_2$ must lie on $\mathbf{F}\mathbf{p}_2$. The fundamental matrix of two rectified images is characterized by the following proposition

Proposition 1 *Two images $\mathbf{I}_1$ and $\mathbf{I}_2$ are rectified iff the fundamental matrix they identify is of the form*

$$\mathbf{F} = \begin{bmatrix} 0 & 0 & 0 \\ 0 & 0 & -1 \\ 0 & 1 & 0 \end{bmatrix}. \tag{2}$$

Proof: If the images are rectified, the epipoles are

$$\mathbf{e}_1 = \mathbf{e}_2 = \begin{bmatrix} 1 \\ 0 \\ 0 \end{bmatrix}. \tag{3}$$

If $\mathbf{p}_2 = [X, Y, Z]^t$ we have that $\mathbf{F}\mathbf{p}_2 = [0, 1, -Y]^t$, and therefore $\mathbf{M}\mathbf{p}_2 = [x, Y, 1]^t$. It is evident that in such case $\mathbf{M}$ can be chosen as the identity. Consequently, for a pair of rectified images we have $\mathbf{F} = [\mathbf{e}_1]_\times$, that is $\mathbf{F}$ is of the form given in (2).

Conversely if two images identify the fundamental matrix given in (2) and $[x_1, y_1, 1]^t$ and $[x_2, y_2, 1]^t$ are a couple of correspondent points, because of (1) it is that $y_1 - y_2 = 0$. Therefore the two images are rectified. ■

3 The class of rectifying homographies

Let us call $\mathbf{H}_1$ and $\mathbf{H}_2$ the two homographies rectifying $\mathbf{I}_1$ and $\mathbf{I}_2$, respectively. The pair of rectifying homographies is not unique; in general, some rectifying homographies are unacceptable, for instance as they cause too large projective distortions (e.g., some points can be mapped to infinity). It is therefore necessary to constrain any algorithm computing $\mathbf{H}_1$ and $\mathbf{H}_2$ in such a way that the rectified images do not look too different from the original ones.

Hartley [8] uses the conditions that one of the two homographies, say $\mathbf{H}_2$, should be close to a rigid transformation in the neighborhood of a selected point $\mathbf{p}_0$. He shows that, in this case, $\mathbf{H}_2$ can be conveniently written as

$$\mathbf{H}_2 = \mathbf{K}\mathbf{R}\mathbf{T}, \tag{4}$$

where $\mathbf{T}$ is a translation taking $\mathbf{p}_0$ to the origin, $\mathbf{R}$ is a rotation mapping the epipole (which is assumed known) to a point $[1, 0, f]^t$ on the x axis, and $\mathbf{K}$ is a transformation mapping $[1, 0, f]^t$ to $[1, 0, 0]^t$ and acting as the identity map close to the origin. In particular, $\mathbf{K}$ is given by the matrix

$$\mathbf{K} = \begin{bmatrix} 1 & 0 & 0 \\ 0 & 1 & 0 \\ -f & 0 & 1 \end{bmatrix} \tag{5}$$

In this way, the homography $\mathbf{H}_2$ depends only on two parameters: f and the angle of rotation, θ. If we discard the translation, i.e. consider the data have been already scaled by mean of $\mathbf{T}$, then $\mathbf{H}_2$ is of the form

$$\begin{bmatrix} \cos\theta & \sin\theta & 0 \\ -\sin\theta & \cos\theta & 0 \\ -f\cos\theta & -f\sin\theta & 1 \end{bmatrix}$$

It is proven in [8] that if $\mathbf{H}_2$ is given and the fundamental matrix is factorized as $[\mathbf{e}_1]_\times \mathbf{M}$, then $\mathbf{H}_1$ has the form

$$(\mathbf{I} + [1, 0, 0]^t \mathbf{a}^t)\mathbf{H}_2\mathbf{M} \tag{6}$$

for some vector $\mathbf{a}$, then $\mathbf{H}_1$ is not uniquely determined by $\mathbf{H}_2$. If we do some algebra on equation (6) it turns out that the free entries of $\mathbf{H}_1$ are the three elements on the first row, as anyone would expect. In fact it is

$$\mathbf{H}_1 = \begin{bmatrix} a & b & c \\ 0 & 1 & 0 \\ 0 & 0 & 1 \end{bmatrix} \mathbf{H}_2\mathbf{M}$$

The two homographies are identified up to a scale factor. Since we can assume that the point $[0,0,1]^t$ (i.e. the origin of the images reference frames) is mapped by $\mathbf{H}_1$ and $\mathbf{H}_1$ to finite points, we can fix $\mathbf{H}_1(3,3) = \mathbf{H}_2(3,3) = 1$.

4 The rectification algorithm

Let us assume that N point correspondences between the two images $\mathbf{I}_1$ and $\mathbf{I}_2$ are determined. Let $\mathbf{p}_{ij}$ be the i-th point in the image $\mathbf{I}_j$.

The idea of the rectification algorithm presented in this paper is to find two homographies $\mathbf{H}_1$ and $\mathbf{H}_2$ such that

$$(\mathbf{H}_2\mathbf{p}_{i2})^t\mathbf{F}\mathbf{H}_1\mathbf{p}_{i1} = 0 \tag{7}$$

for each $i = 1, \cdots, N$, where $\mathbf{F}$ is the one given in equation (2). In this way, because of proposition 1 we are sure that the two warped images $\mathbf{H}_1(\mathbf{I}_1)$ and $\mathbf{H}_2(\mathbf{I}_2)$ are rectified. The two homographies are then estimated by minimizing the objective function

$$\mathcal{F}(\mathbf{H}_1, \mathbf{H}_2) = \sum_{i=1}^{N} [(\mathbf{H}_2\mathbf{p}_{i2})^t\mathbf{F}\mathbf{H}_1\mathbf{p}_{i1}]^2 \tag{8}$$

Note that the above function $\mathcal{F}(\mathbf{H}_1, \mathbf{H}_2)$ (7) involves only the second and third rows of the unknown matrices. While this is sufficient to estimate the two parameters f and θ, a further step is necessary in order to fix the remaining entries on the first row of $\mathbf{H}_1$. This is consistent with equation (6).

Since the two rectified images should not look too different, the first row of $\mathbf{H}_1$ can be uniquely determined by minimizing the sum of squared distances

$$\sum_{i=1}^{N} [(\mathbf{H}_1\mathbf{p}_{1i})_x - (\mathbf{H}_2\mathbf{p}_{2i})_x]^2. \tag{9}$$

This is a simple, *linear* least-squares problem, which can be solved in closed form (see Strang [20]).

The knowledge of the two rectifying homographies $\mathbf{H}_1$ and $\mathbf{H}_2$ gives the epipoles $\mathbf{e}_1$ and $\mathbf{e}_2$ of the two original images, since it is $\mathbf{H}_i^{-1}[1,0,0]^t = \mathbf{e}_i$, $i = 1,2$. Moreover, $\mathbf{H}_1$ and $\mathbf{H}_2$ are such that $\mathbf{H}_1^t\mathbf{F}\mathbf{H}_2$ is the fundamental matrix between the two original images. Therefore the method returns also a complete estimation of the epipolar geometry between the two original images, which is implied by the knowledge of 8 point correspondences at least.

The function $\mathcal{F}(\mathbf{H}_1, \mathbf{H}_2)$ is clearly non linear, so we perform the minimization using the Levenberg-Marquardt algorithm [13]. A good initial estimate is important to guarantee the convergence to a right solution.

If we suppose that the two epipoles are far from the images, which is a quite usual situation, a good first approximation is given by considering the two epipoles being at infinity, i.e. the two transformations are considered as affine. We then find the two affine transformations minimizing the cost function

$$\mathcal{G}(\mathbf{H}_1, \mathbf{H}_2) = \sum_{i=1}^{N} [(\mathbf{H}_1\mathbf{p}_{1i})_y - (\mathbf{H}_2\mathbf{p}_{2i})_y]^2 \tag{10}$$

Note that this implies we are assuming $f = 0$. In this hypothesis it is more convenient to write $\mathbf{H}_2$ in the form

$$\begin{bmatrix} a & b & 0 \\ -b & a & 0 \\ 0 & 0 & 1 \end{bmatrix}$$

with the constraint $a^2 + b^2 = 1$. So, $\mathbf{H}_2$ reduces to a simple rotation. Then the minimization problem given in (10) becomes a constrained linear least-square problem (see Golub and van Loan [6]), since a rotation matrix (the one determined by the angle θ) has to be determined.

The two transformations determined in this way are used as starting point for the iterative minimization of $\mathcal{F}(\mathbf{H}_1, \mathbf{H}_2)$.

4.1 The robustness issue

The algorithm described in the previous section involves the solution of least squares minimizations. Least squares estimators assume that each data is corrupted by an independent zero-mean Gaussian noise. If some data do not satisfy this assumptions, they are called *outliers*, while the good data are called *inliers*. Outliers in our case can be generated by a bad localization of the point in the images or by false matches. It is well known that even when the data contains only one outlier, a least-squares estimate may be seriously perturbed [16]. For these reason in the last few decades more robust estimation methods have been developed (see [11] for a review of the most used estimators in computer vision).

In order to make our implementation robust to the presence of wrong point correspondences we included an outlier detector step, based on the Least Median of Squares (LMS) paradigm [16], which can theoretically tolerate 0.5 of data corruption, by looking for the parameter set which minimizes a robust error measure for the model to estimate. A brief description of the LMS paradigm is given in the appendix. In our case the model is the solution of (10). Note that in doing that we assume that the affine transformation is a correct model, in other words we assume that the rotation between the two cameras is not large. If this assumption is not valid the outlier detector can fail, including some wrong matches among the inliers, if the fraction of outliers is large.

Since LMS discriminate between outliers and inliers on the basis of an instance of the model computed from a minimum set of data, it is possible that few inliers are discarded as outliers, as already observed in [15]. This is not a problem if we deal with a large amount of data, but if our set of point correspondences is small it is important to maintain as many inliers as possible. The general idea to recover inliers is to measure the influence of each potential outliers on the Least Squares estimation of the model: if a point is an outlier the influence will be high.

In order to do so we used the following second step. An estimation M of the model is computed using all the inliers detected by the LMS, and from this estimation the standard deviation σ of the residuals (see appendix) of the inliers is obtained. Then we compute the residual r from M for each potential outlier, and if $r < 2.5\sigma$ we retain the point as inlier, otherwise it is definitively discarded.

More sophisticated statistical methods, like the one described in [1], have not been used because more computationally expensive.

5 Experimental results

The algorithm has been tested on several stereo pairs, and the results proved to be quite satisfactory. Here we report the results obtained running our algorithm on four stereo pairs available from the INRIA-Syntim web site (see acknowledgements section). For all the three cases a small number of point correspondences have been determined manually, so that the accuracy of the correspondences is limited.

For the first stereo pair, called *Tot*, 16 point correspondences have been selected, and 2 of them are real outliers. The LMS detect 6 point matches as outliers in total. Therefore 4 good matches are discarded. The second step of the outlier detector recover 3 good matches, so that, in the end, only 1 good match is lost, while all the outliers are detected. In Figure 1 the results of the experiments are shown.

In the second stereo pair, *Rubik*, again 16 point correspondences have been selected, and 3 of them are outliers. The LMS returns 6 points out of the 16 as outliers, while the second step of our outlier detector recover all the inliers discarded by the LMS, so that in the end only the 3 outliers are discarded. Results of this experiments are shown in Figure 2.

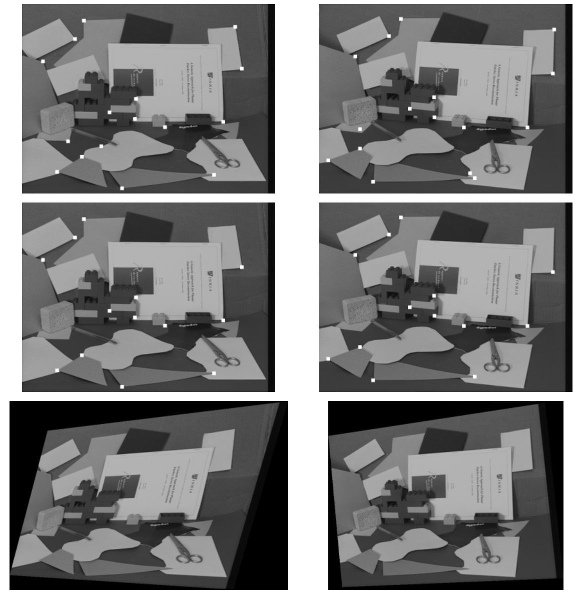

Fig. 1. Tot stereo pair. Top row: original images with all the 16 point correspondences superimposed, two of them are wrong matches. Middle row: original images with the 13 inliers detected by the outlier detector; only a good match is lost. The LMS had detected only 10 inliers, the other 3 good correspondences have been recovered by the second authentication step. Bottom row: the two rectified images

For the the third stereo pair, *Balmire*, the point correspondences selected are 22, and the outliers included are 3. The LMS detect 8 points as outliers, 4 inliers out of the 8 discarded are recovered by the last step of the outlier detector. In the end all the outliers are detected and only 1 inlier is discarded. The results of this experiment are shown in Figure 3.

For the last stereo pair, *Books*, we selected 19 point correspondences, and three of them are wrong matches. This time the LMS detected all the 16 inliers correctly. The results of this experiment are shown in Figure 4.

6 Conclusions

A robust algorithm for performing uncalibrated rectification between a pair of stereo images has been described in this paper. The difference with respect the few works on uncalibrated rectification is that the method does not require a previous estimation of the epipolar geometry. It might be observed that the core of the algorithm is a non-linear minimization, while the rectification algorithms based on recovery of the fundamental matrix are all linear. However as remarked in [8], linear algorithms estimating $\mathbf{F}$ are numerically unstable, and the best results are obtained using an iterative process. Therefore our algorithm is ultimately not more computationally expensive than the previous ones. The algorithm has been made robust and reliable by mean of

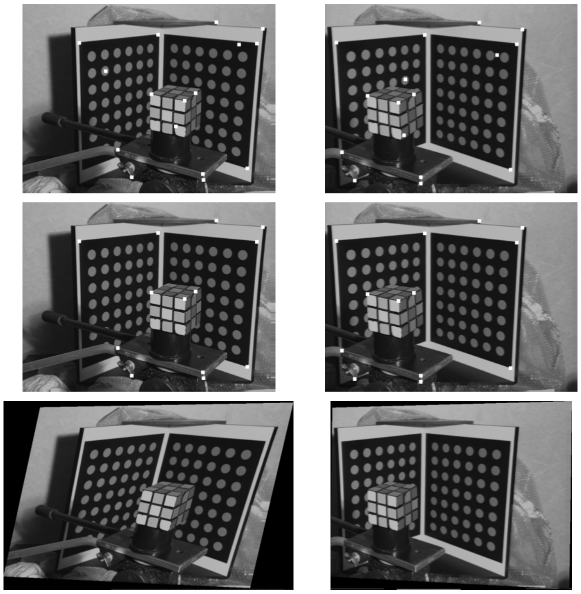

Fig. 2. Rubik stereo pair. Top row: original images with all the 16 point correspondences superimposed, 3 of them are wrong matches. Middle row: original images with the 13 inliers detected by the outlier detector; no good matches are lost. The LMS had detected only 10 inliers, the other 3 good correspondences have been recovered by the second authentication step. Bottom row: the two rectified images

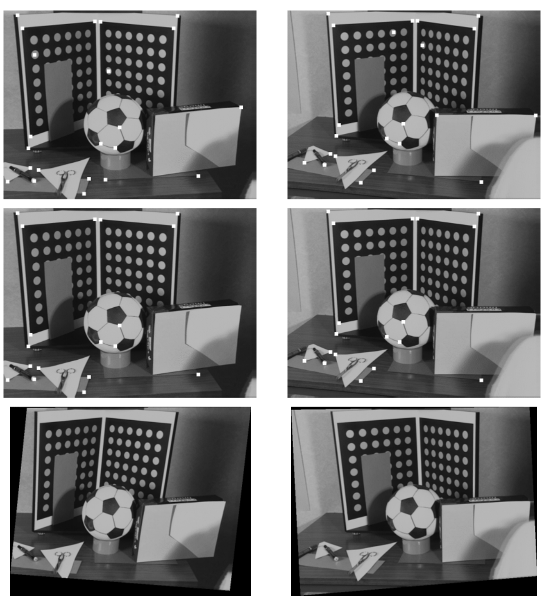

Fig. 3. Balmire stereo pair. Top row: original images with all the 22 point correspondences superimposed, 3 of them are wrong matches. Middle row: original images with the 18 inliers detected by the outlier detector; only 1 good match is lost. The LMS had detected only 14 inliers, the other 4 good correspondences have been recovered by the second authentication step. Bottom row: the two rectified images

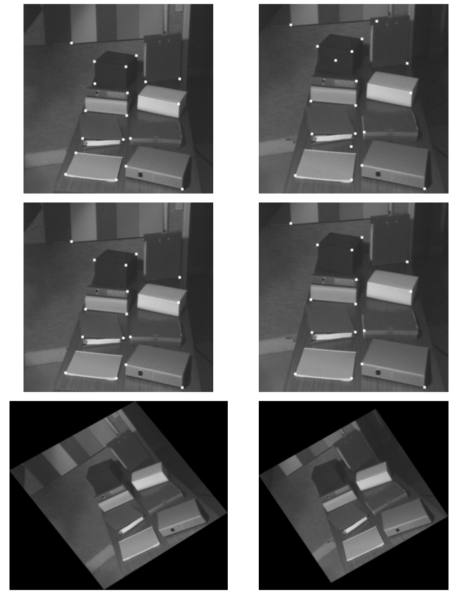

Fig. 4. Books stereo pair. Top row: original images with all the 19 point correspondences superimposed, 3 of them are wrong matches. Middle row: original images with the 16 inliers detected by the outlier detector; no good match is lost. The LMS had detected all the 16 inliers. Bottom row: the two rectified images

a two steps outliers detector, based on the classic Least Median of Square estimator, which reduces the number of good matches discarded . The experimental results show that the algorithm performs well in presence of outliers, and with noisy point correspondences.

Acknowledgements

The real stereo pairs shown in this paper are available from INRIA-Syntim under Copyright (http://www-syntim.inria.fr/syntim/analyse/paires-eng.html).

A The Least Median of Squares estimator

In this section we give a short description of the Least Median of Squares estimator. For a more detailed discussion on the topic we refer the reader to [16].

Let us suppose that the model we have to estimate from a set of data points $mathbfp_i$ is the vector $\mathbf{b}$, solution of equation $F(\mathbf{p}_i, \mathbf{b}) = 0$. Given a set of parameters $\hat{\mathbf{b}}$ we introduce $r_i = F(\mathbf{p}_i, \hat{\mathbf{b}})$, usually called *residual*. LMS finds a parameter vector which minimizes the objective function

$$\operatorname*{med}_i r_i^2$$

over a set of random subsamples of the data set.

Let us suppose that p is the minimum number of observations needed to estimate the model. Two point matches suffice in our case to give a closed-form solution. The algorithm randomly selects a subset of p observations and uses only them to estimate the model. For each estimated model, the median of the square of the residuals is computed, and the temporary best model is considered the one which minimizes the objective function. Ideally the trials should be run on *each* subset of p observations, but this is usually computationally impossible. Thus the number m of trials is chosen in such a way to have a probability Υ that a subsample without any outlier has been included in our selection. The expression for this probability is $\Upsilon = 1 - (1 - (1 - \epsilon)^p)^m$, where ϵ is the fraction of data consisting of outlier; m can be determined for given values of ϵ, p and Υ

$$m = \frac{\log(1 - \Upsilon)}{\log(1 - (1 - \epsilon)^p)}.$$

If we assume $\epsilon = 0.5, \Upsilon = 0.99$, and $p = 5$ we get $m = 145$, and these are the values we used in our experiments.

Once this model is estimated, a robust standard deviation is computed using the formula

$$\hat{\sigma} = 1.4826 \left(1 + \frac{5}{n - p}\right) \operatorname*{med}_i \sqrt{r_i^2}$$

suggested by Rousseeuw in [16]. Then the outlier are detected using the following binary weight function

$$w_i = \begin{cases} 1 & \frac{\|r_i\|}{\hat{\sigma}} \leq 2.5 \\ 0 & \frac{\|r_i\|}{\hat{\sigma}} > 2.5 \end{cases}.$$

The data points having $w_i = 1$ are inliers, that is they belong to the assumed model. Points having $w_i = 0$ are considered as outlier and removed from the data set. Finally all the estimated inliers are used to estimate the model using Least Squares, in order to have a more accurate estimation.

References

[1] A. C. Atkinson. Masking unmasked. *Biometrika*, 73(3):533–541, 1986.

[2] N. Ayache. *Artificial vision for mobile robots: stereo vision and multisensory perception*. The MIT Press, 1991.

[3] N. Ayache and C. Hansen. Rectification of images for binocular and trinocular stereovision. In *Proceedings of the International Conference on Pattern Recognition*, pages 11–16, 1988.

[4] O. Faugeras. *Three-Dimensional computer vision: a geometric viewpoint*. MIT Press, 1993.

[5] A. Fusiello, E. Trucco, and A. Verri. Rectification with unconstrained stereo geometry. In *Proceedings of British Machine Vision Conference*, pages 400–409, 1997.

[6] G. H. Golub and C. F. Van Loan. *Matrix computations*. The John Hopkins University Press, 3rd edition, 1996.

[7] R. I. Hartley. In defense of the eight-point algorithm. *IEEE Transactions on Pattern Analysis and Machine Intelligence*, 19(6), 1997.

[8] R. I. Hartley. Theory and practice of projective rectification. *International Journal of Computer Vision, to appear*, 1998.

[9] F. Isgrò and E. Trucco. Projective rectification without epipolar geometry. In *Proceedings of the IEEE International Conference on Computer Vision*, volume 1, pages 94–99, 1999.

[10] Q. T. Luong and O. D. Faugeras. The Fundamental matrix: theory, algorithms, and stability analysis. *International Journal of Computer Vision*, 17(1):43–76, 1996.

[11] P. Meer, D. Mintz, A. Rosenfeld, and D. Y. Kim. Robust regression methods for computer vision: a review. *International Journal of Computer Vision*, 6(1):59–70, 1991.

[12] D. Papadimitriou and T. Dennis. Epipolar line estimation and rectification for stereo image pairs. *IEEE Transactions on Image Processing*, 5(4):672–676, April 1996.

[13] W. H. Press, S. A. Teukolsky, W. T. Vetterling, and B. P. Flannery. *Numerical recipes in C: the art of scientific computing*. Cambridge University Press, 2nd edition, 1992.

[14] L. Robert, C. Zeller, O. Faugeras, and M. Hebert. Applications of non-metric vision to some visually guided robotics tasks. In Y. Aloimonos, editor, *Visual navigation: from biological systems to unmanned ground vehicles*, chapter 5, pages 89–134. Lawrence Erlbaum Associates, 1997.

[15] P. J. Rousseeuw. Least median of squares regression. *Journal of American Statistical Association*, 79(388):871–880, December 1984.

[16] P. J. Rousseeuw and A. M. Leroy. *Robust regression and outlier detection*. Wiley Series in Probability and Mathematical Statistics. Wiley: New York, 1987.

[17] S. M. Seitz and C. R. Dyer. View morphing. In *Proceedings of SIGRAPH96*, pages 21–30, 1996.

[18] J. G. Semple and G. T. Kneebone. *Algebraic projective geometry*. Oxford University Press, 1952.

[19] C. C. Slama, editor. *Manual of photogrammetry*. American Society of Photogrammetry, 1980.

[20] G. Strang. *Linear Algebra and its applications*. Academic Press, 2 edition, 1980.

[21] G. Wolberg. *Digital image warping*. IEEE Computer Society Press, 1990.

[22] Z. Zhang. Determining the epipolar geometry and its uncertainty: a review. *International Journal of Computer Vision*, 27(2):161–195, March 1998.